

Rheology of a Supercooled Polymer Melt

Ryoichi Yamamoto and Akira Onuki

Department of Physics, Kyoto University, Kyoto 606-8502, Japan

(November 5, 2018)

Molecular dynamics simulations are performed for a polymer melt composed of short chains in quiescent and sheared conditions. The stress relaxation function $G(t)$ exhibits a stretched exponential form in a relatively early stage and ultimately follows the Rouse function in quiescent supercooled state. Transient stress evolution after application of shear obeys the linear growth $\int_0^t dt' G(t')$ for strain less than 0.1 and then saturates into a non-Newtonian viscosity. In steady states, strong shear-thinning and elongation of chains into ellipsoidal shapes are found at extremely small shear. A glassy component of the stress is much enhanced in these examples.

PACS numbers: 83.10.Nn, 83.20.Jp, 83.50.By, 64.70.Pf

Stress and dielectric relaxations of glassy polymer melts occur from microscopic to macroscopic time scales in very complicated manners [1,2]. Experiments have shown that the stress relaxation function $G(t)$ exhibits a glassy stretched exponential decay, a glass-rubber transition, a rubbery plateau, and a terminal decay, in this order over many decades of time. Such hierarchical relaxation behavior arises from rearrangements of jammed atomic configurations and subsequent evolution of chain conformations described by the Rouse or reptation dynamics [3,4]. The stress-optical relation between birefringence and stress has also been reported to be violated as the temperature T is approached the glass transition temperature T_g [5–7], obviously owing to enhancement of a glassy part of the stress.

Recent simulations on glassy polymer melts have mainly treated self-motions of particles in quiescent states [8–10]. However, not enough theoretical efforts have been made on the rheological properties of glassy polymers. Hence, we will first study linear rheology of a model short chain system via very long molecular dynamics simulations. Then, we will demonstrate that chains are very easily elongated at extremely small shear rate $\dot{\gamma}$ on the order of the inverse Rouse time. Marked shear-thinning behavior then takes place for larger shear rates, indicating a decrease of the monomeric friction among different chains. On the other hand, in supercooled simple fluid mixtures [11], the shear-dependent structural rearrangement time $\tau_b(\dot{\gamma})$ depends on shear as $\tau_b(\dot{\gamma})^{-1} = \tau_b(0)^{-1} + A_b \dot{\gamma}$, where A_b is of order 1 and $\tau_b(0)$ is on the order of the so-called α relaxation time τ_α obtained from the incoherent van Hove time correlation function. The steady state viscosity is expressed in a very simple form, $\eta(\dot{\gamma}) = A_\eta \tau_b(\dot{\gamma}) + \eta_B$, for any T and $\dot{\gamma}$, where A_η and η_B are constants. We have also found that the cage breakage occurs collectively in the form of clusters characterized by a correlation length ξ [12], where the dynamic scaling $\tau_b(\dot{\gamma}) \sim \xi^2$ holds in three dimensions.

In our model all the bead particles interact with a Lennard-Jones potential of the form [4,8,10], $U_{LJ}(r) =$

$4\epsilon[(\sigma/r)^{12} - (\sigma/r)^6] + \epsilon$. It is cut off at the minimum distance $2^{1/6}\sigma$, so we use its repulsive part only to prevent spatial overlap of particles. Consecutive beads on each chain are connected by an anharmonic spring of the form, $U_F(r) = -\frac{1}{2}k_c R_0^2 \ln[1 - (r/R_0)^2]$ with $k_c = 30\epsilon/\sigma^2$ and $R_0 = 1.5\sigma$, so the bond length cannot exceed R_0 . In a cubic box with length $L = 10\sigma$ under the periodic boundary condition, we put $M = 100$ chains composed of $N = 10$ beads. The number density is fixed at a very high value of $n = NM/V = 1/\sigma^3$, which results in severely jammed configurations at low T . We will measure space and time in units of σ and $\tau_0 = (m\sigma^2/\epsilon)^{1/2}$ with m being the mass of a bead. The temperature T will be measured in units of ϵ/k_B . Simulations were performed in normal ($T = 1.0$) and supercooled ($T = 0.4$ and 0.2) states with and without shear. The bond lengths $b_j = |\mathbf{R}_j - \mathbf{R}_{j+1}|$ between consecutive beads on each chain exhibit only small deviations on the order of a few % from $b_0 \cong 0.96$, which gives the minimum of $U_{LJ}(r) + U_F(r)$, for any T and $\dot{\gamma}$ in our study. Thus the bond lengths are nearly fixed in our model system.

We took data after long equilibration periods (10^6 at $T = 0.2$) to suppress aging (slow equilibration) effects in various quantities such as the pressure or the density time correlation functions. At zero shear we imposed the micro-canonical condition with the time step $\Delta t = 0.005$. In order to obtain accurate linear viscoelastic behavior, very long simulations of order $10^2 \tau_R$ were performed, where τ_R is the primary Rouse relaxation time. In the literature [4,8,10], simulation times have been typically up to τ_R in supercooled states. In the presence of shear we set $\Delta t = 0.0025$ and kept the temperature at a constant using the Gaussian constraint thermostat to eliminate viscous heating. After a long equilibration time in a quiescent state for $t < 0$, all the particles acquired the average flow velocity $\dot{\gamma}y$ in the x direction at $t = 0$ and then the Lee-Edwards boundary condition [13,14] maintained the simple shear flow. Steady sheared states were realized after transient viscoelastic behavior.

As has been confirmed in the literature [8–10], the

dynamics in quiescent supercooled states is reasonably well described by the Rouse model, where the relaxation time of the p th mode of a chain is expressed as $\tau_p = \zeta b^2 / [12k_B T \sin^2(p\pi/2N)]$ ($p = 1, \dots, N-1$) [15]. Here, the statistical segment length b is related to the variance of the end-to-end vector of a chain $\mathbf{P} = \mathbf{R}_N - \mathbf{R}_1$ by $b = [(\mathbf{P}^2)/(N-1)]^{1/2}$, which is 1.17, 1.18, 1.19 for $T = 1.0, 0.4, 0.2$, respectively. We determined the monomer friction constant ζ from the relaxation $\langle \mathbf{P}(t) \cdot \mathbf{P}(0) \rangle = 2N^{-1} \sum_{\ell=0,1,\dots} \cot^2(\pi(2\ell+1)/2N) \exp(-t/\tau_{2\ell+1})$ of the end-to-end vector. The Rouse relaxation time $\tau_R (= \tau_1 \cong \zeta b^2 N^2 / 3\pi^2 k_B T)$ then increases drastically with lowering T as $\tau_R = 250, 1800$, and 6×10^4 for $T = 1.0, 0.4, 0.2$, respectively. We also calculated the α relaxation time τ_α from $F_q(\tau_\alpha) = e^{-1}$ at $q = 2\pi$ [8], where $F_q(t) = \sum_{j=1}^N \langle \exp[i\mathbf{q} \cdot (\mathbf{R}_j(t) - \mathbf{R}_j(0))] \rangle / N$ is the van Hove self-correlation function for the displacement of a tagged particle. Then we obtained the result $\tau_\alpha \cong 0.017 \zeta b^2 / k_B T$ at any T , so we have $\tau_R \cong 2N^2 \tau_\alpha$ in our system.

Now let us discuss the linear viscoelastic behavior in supercooled states. In Fig.1 we show the stress relaxation function,

$$G(t) = \langle \sigma_{xy}^T(t) \sigma_{xy}^T(0) \rangle / V k_B T, \quad (1)$$

where σ_{xy}^T is the space integral of the xy component of the total stress tensor over the volume $V = L^3$. At the lowest temperature $T = 0.2$, $G(t)$ exhibits salient features of glassy polymer melts [1,2]. Its initial value is of order 100 (in units of ϵ/σ^3) and is very large, and it relaxes to a value G_0 about 5 for $t \gtrsim 1$. We then have a slow decay of the form,

$$G(t) \cong G_0 \exp[-(t/\tau_s)^\beta], \quad (2)$$

where $\tau_s = 90 \sim \tau_\alpha$ and $\beta = 0.5$. The agreement to Eq.(2) is excellent for $1 \lesssim t \lesssim 10\tau_s$. This glassy behavior arises from monomeric structural relaxation. For $t \gtrsim 50\tau_s$ it approaches the Rouse stress relaxation function,

$$G_R(t) = n k_B T N^{-1} \sum_{p=1}^{N-1} \exp(-2t/\tau_p), \quad (3)$$

which is equal to $T(N-1)/N$ for $t \lesssim \tau_\alpha$ and decays as $TN^{-1} \exp(-2t/\tau_R)$ for $t \gg \tau_R$ in the dimensionless units. Obviously, this final stage behavior arises from relaxation of large scale chain conformations. The crossover between these two regions occurs in a narrow time range in our case. Experimentally, however, the intermediate region, which connects the glassy and polymeric (Rouse or reptation) relaxations, extends over a much wider time range (typically 4 decades [1]), and $G(t)$ there has been fitted to an algebraic form, $G(t) \cong e^{-1} G_0 (t/\tau_s)^{-a}$ with $a \sim 0.5$ [1,2]. In addition, with increasing the molecular weight, a rubbery plateau has been observed to develop after the crossover before

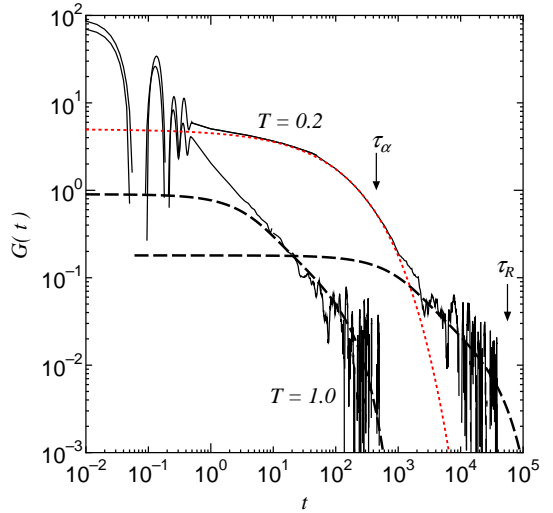


FIG. 1. The stress relaxation function $G(t)$ (thin-solid lines) at $T = 0.2$ in a supercooled state and $T = 1$ in a normal liquid state. It may be fitted to the stretched exponential form (dotted line) at relatively short times and tends to the Rouse relaxation function $G_R(t)$ (bold-dashed lines) at long times.

the terminal decay, whereas it is not apparently seen in our short chain system. In our case, the (zero-frequency) linear viscosity η consists of a monomeric part $\Delta\eta$ of order $10\tau_s$ from the integration in the time region $t \lesssim 10\tau_s$ and the Rouse viscosity $\eta_R = \int_0^\infty dt G_R(t) \cong 0.808TN^{-1}\tau_R$ from $t \gtrsim \tau_R$. The ratio $\Delta\eta/\eta_R$ is thus of order $1/(TN)$ (~ 1 at $T = 0.2$), whereas we should have $\Delta\eta \ll \eta_R$ for much larger N .

In the Rouse model, the space integral of the polymer (entropic) stress $\sigma_{\alpha\beta}^R$ is the sum of $k_B T b_{j\alpha} b_{j\beta} / b^2$ over all the bonds in the system, where $b_{j\alpha}$ are the Cartesian components of the bond vectors $\mathbf{b}_j = \mathbf{R}_{j+1} - \mathbf{R}_j$. We have confirmed that the relaxation function $G_c(t) = \langle \sigma_{xy}^R(t) \sigma_{xy}^R(0) \rangle / V k_B T$ nearly coincides with $G_R(t) \cong G(t)$ for $t \gtrsim 0.1\tau_R$, whereas it is about a half of $G_R(t)$ for $t \lesssim \tau_s$. We note that the bond vectors have the nearly fixed length $b_0 \cong 0.96$, and a bond orientation tensor $Q_{\alpha\beta}$ may be defined as

$$Q_{\alpha\beta} = (N-1)^{-1} \sum_{j=1}^{N-1} \langle b_{j\alpha} b_{j\beta} \rangle / b_0^2. \quad (4)$$

Then we have $Q_{\alpha\beta} \propto \langle \sigma_{\alpha\beta}^R \rangle$. If the electric polarizability tensor of a bead is uniaxial along the bond vector, the deviation of the dielectric tensor $\Delta\epsilon_{\alpha\beta}$ is proportional to $Q_{\alpha\beta} - \delta_{\alpha\beta}/3$. In flow birefringence we have,

$$\Delta\epsilon_{xy} = C \langle \sigma_{xy}^R \rangle / V, \quad (5)$$

where C is a constant. In supercooled states $\langle \sigma_{xy}^R \rangle / V$ can be much smaller than the total shear stress σ_{xy} , for instance, in transient states or in oscillatory shear.

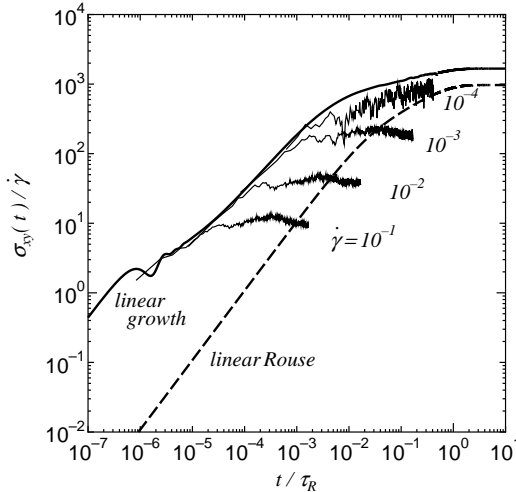


FIG. 2. Shear stress divided by shear rate $\dot{\gamma} = 10^{-1}, 10^{-2}, 10^{-3}, 10^{-4}$ (thin-solid lines) vs t/τ_R (where $\tau_R = 6 \times 10^4$) at $T = 0.2$. The curves follow the linear growth function (bold-solid line) for $\dot{\gamma}t \lesssim 0.1$, but afterwards depart from it. The linear growth function in the Rouse model is also plotted(bold-dashed line).

Therefore, the usual stress-optical law $\Delta\varepsilon_{xy} = C\sigma_{xy}$, which is valid far above T_g , breaks down close to T_g .

In Fig.2 we show the stress growth function $\sigma_{xy}(t)/\dot{\gamma}$ after application of shear at $t = 0$ at the lowest temperature $T = 0.2$ for various $\dot{\gamma}$. The curves are the averages of data of eight independent runs. In the initial stage, in which $\dot{\gamma}t \lesssim 0.1$, we can see the linear viscoelastic growth, $\sigma_{xy}(t)/\dot{\gamma} = \int_0^t G(t')dt'$, whereas a nonlinear regime sets in for $\dot{\gamma}t \gtrsim 0.1$, resulting in the non-Newtonian viscosity $\eta(\dot{\gamma})$. As a guide, we also plot the linear growth function $\int_0^t G_R(t')dt'$ from the Rouse model, which is much smaller than the true linear growth for $t \ll \tau_R$. The relevant physical processes are as follows: For $\dot{\gamma}t \lesssim 0.1$ the overall chain conformations are affinely deformed, whereas for $\dot{\gamma}t \gtrsim 0.1$ the structural rearrangements among beads belonging to different chains become appreciably induced by shear (as in the case of supercooled simple fluids [11]). Experimentally, a stress overshoot (a rounded maximum of $\sigma_{xy}(t)$) has been observed at $\dot{\gamma}t = 0.05 - 0.1$ for higher molecular weight melts close to T_g [1].

In Fig.3 we display the steady state viscosity $\eta(\dot{\gamma})$ at $T = 0.2, 0.4$, and 1 . It exhibits marked shear-thinning behavior for $\dot{\gamma}\tau_R \gtrsim 1$ and becomes independent of T for very high shear rates. The horizontal arrows indicate the linear viscosity from the Rouse model η_R , and the vertical arrows indicate the points at which $\dot{\gamma} = \tau_R^{-1}$. In particular, the curve of $T = 0.2$ may be fitted to $\eta \propto \dot{\gamma}^{-\nu}$ with $\nu \simeq 0.7$ for $\dot{\gamma}\tau_R \gtrsim 1$. Similar shear-thinning has been reported in MD simulations of short chain systems in normal liquid states, but at much higher shear rates [16,17]. In the case of supercooled simple fluid mixtures [11], shear-thinning becomes apparent for $\dot{\gamma} \gtrsim 0.1\tau_\alpha^{-1}$.

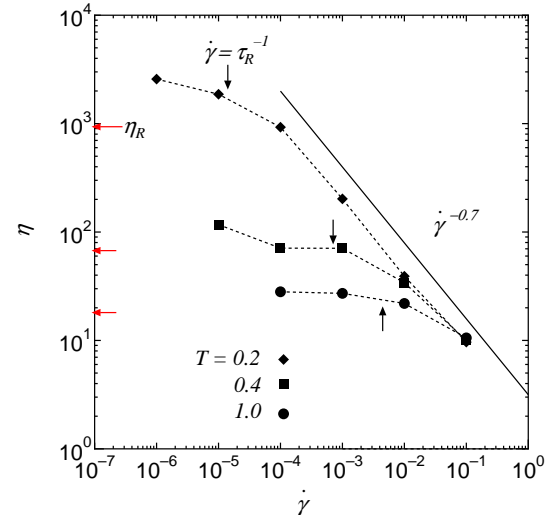


FIG. 3. The steady state viscosity vs $\dot{\gamma}$ for $T = 0.2, 0.4, 1$. A line of slope -0.7 is also written as a view guide.

In the present short chain system, significant shear-thinning occurs at much smaller shear of order $\tau_R^{-1} \sim \tau_\alpha^{-1} N^{-2}$. At this early onset, the overall elongation of chains take place, as will become evident in Fig.5 below. It is worth noting that the shear stress at $\dot{\gamma} \sim \tau_R^{-1}$ is of order $nk_B T/N$ (which would be the modulus in the rubbery plateau for longer chain systems).

We finally examine anisotropy in the chain conformations in shear at $T = 0.2$ and $\dot{\gamma} = 10^{-4}$. In Fig.4 (a), we plot the xy cross section ($z = 0$) of the steady state bead distribution function,

$$g_s(\mathbf{r}) = N^{-1} \sum_{j=1}^N \langle \delta(\mathbf{R}_j - \mathbf{R}_G - \mathbf{r}) \rangle, \quad (6)$$

where $\mathbf{R}_G(t) = N^{-1} \sum_{n=1}^N \mathbf{R}_n(t)$ is the center of mass of a chain. In Fig.4 (b), we plot the structure factor,

$$S(\mathbf{q}) = N^{-2} \sum_{i,j=1}^N \langle \exp(i\mathbf{q} \cdot (\mathbf{R}_i - \mathbf{R}_j)) \rangle, \quad (7)$$

in the $q_x q_y$ plane ($q_z = 0$). It is proportional to the scattering intensity from labeled chains in shear [18]. We recognize that $g_s(\mathbf{r})$ and $S(\mathbf{q})$ almost saturate into the forms in Fig.4 for $\dot{\gamma} \gtrsim 10/\tau_R$. The figures indicate that our short chains take ellipsoidal shapes on the average once $\dot{\gamma} \gtrsim 10/\tau_R$. The angle θ between the ellipsoids and the y (shear gradient) direction is also written, which is calculated using Eq.(8) below. Let us define the tensor $I_{\alpha\beta} = \sum_{i,j=1}^N \langle (\mathbf{R}_i - \mathbf{R}_j)_\alpha (\mathbf{R}_i - \mathbf{R}_j)_\beta \rangle / N^2$. For small q with $q_z = 0$, we have the expansion,

$$S(\mathbf{q}) = 1 - \frac{1}{2} a_1^2 (\mathbf{q} \cdot \mathbf{e}_1)^2 - \frac{1}{2} a_2^2 (\mathbf{q} \cdot \mathbf{e}_2)^2 + \dots, \quad (8)$$

where $\{\mathbf{e}_1, \mathbf{e}_2\}$ and $\{a_1^2, a_2^2\}$ are the eigen unit vectors and values of the tensor $I_{\alpha\beta}$ with $\alpha, \beta = x, y$. The two lengths a_1 and a_2 are the shorter and longer radii of the

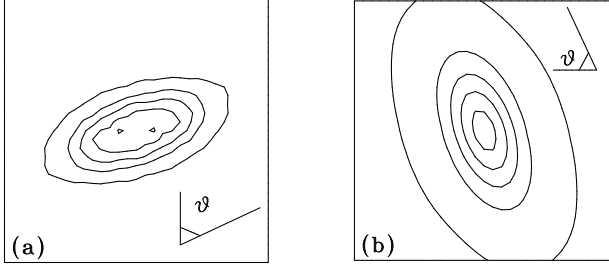


FIG. 4. (a) Isointensity curves of $g_s(\mathbf{r})$ in Eq.(6) in the xy plane ($-3.75 < x, y < 3.75$, $z = 0$). (b) Those of the incoherent structure factor $S(\mathbf{q})$ in Eq.(7) in the $q_x q_y$ plane ($-\pi < q_x, q_y < \pi$, $q_z = 0$). The values on the isolines are $0.01 + 0.02n$ in (a) and $0.1 + 0.2n$ in (b) with $n = 0, 1, \dots, 4$ from outer to inner. Here $T = 0.2$, $\dot{\gamma} = 10^{-4}$, and the flow is in the horizontal (x) direction. The θ is the angle between the average chain shapes and the y axis.

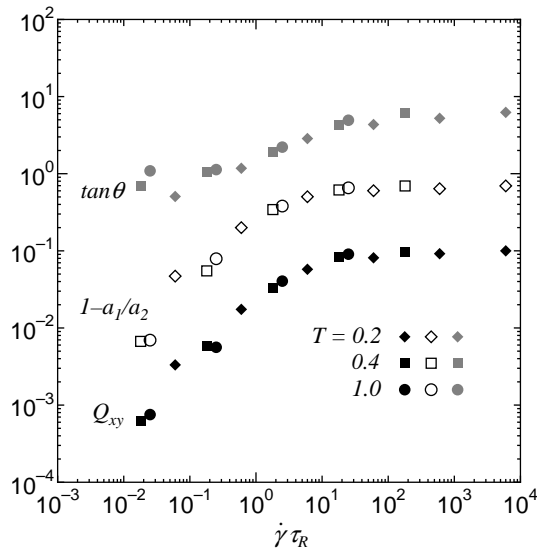


FIG. 5. $\tan \theta$, $1 - a_1/a_2$, and Q_{xy} vs $\dot{\gamma}\tau_R$.

ellipses. In Fig.5 we write $\tan \theta = -e_{1y}/e_{1x}$, the degree of elongation $1 - a_1/a_2$, and the xy component Q_{xy} of the tensor in Eq.(4). For $\dot{\gamma}\tau_R \gtrsim 10$ we have $\theta \cong 80^\circ$, $a_1/a_2 \cong 0.3$, $Q_{xy} \cong 0.1$. These quantities represent the average chain forms and bond orientation and are insensitive to T if plotted vs $\dot{\gamma}\tau_R$. We stress that the shape changes of chains start to occur at $\dot{\gamma} \sim \tau_R^{-1}$ while the monomeric structural relaxation is only slightly affected by shear. In fact, we found that the cage breakage time $\tau_b(\dot{\gamma})$ among neighboring beads belonging to different chains [11] does not change appreciably for $\dot{\gamma} \sim \tau_R^{-1}$ at $T = 0.2$. This tendency should be more evident for longer chain systems.

(i) In our simulations, the stress relaxation function obeys a stretched exponential decay and the Rouse relaxation, although the chain length is too short and the temperature is too high to reproduce the glass-rubber transition region and the rubbery plateau. (ii) We have

also found very early onset of the nonlinear regime of shear. Strong shear-thinning and anisotropic scattering can be predicted for $\dot{\gamma} \gtrsim \tau_R^{-1}$ or for $\sigma_{xy} \gtrsim nk_B T/N$ in the Rouse case $N < N_e$. In the entangled case $N > N_e$ the threshold shear rate and stress needed for the onset of nonlinearity should be of order τ_{rep}^{-1} and $nk_B T/N_e$, respectively, where τ_{rep} is the reptation time. Scattering experiments from very weakly sheared melts near T_g are promising. (iii) Although not presented here, heterogeneities are much enhanced at low T in the cage breakage events among beads belonging to different chains [12]. They are characterized by the correlation length ξ dependent on T and $\dot{\gamma}$. Interesting crossover effects can then be expected at $\xi \sim bN^{1/2}$ for longer chain systems.

This work is supported by Grants in Aid for Scientific Research from the Ministry of Education, Science, Sports and Culture of Japan. Calculations have been performed at the Human Genome Center, Institute of Medical Science, University of Tokyo.

- [1] S. Matsuoka, *Relaxation Phenomena in Polymers*, (Oxford, New York, 1992).
- [2] G.R. Stroble, *The Physics of Polymers*, (Springer, Heidelberg, 1996).
- [3] M. Doi and S.F. Edwards, *The Theory of Polymer Dynamics* (Clarendon, Oxford, 1986).
- [4] K. Kremer and G.S. Grest, *J. Chem. Phys.*, **92** 5057 (1990).
- [5] R. Muller and J.J. Pesce, *Polymer*, **35**, 734 (1994).
- [6] M. Kröger, C. Luap, and R. Muller, *Macromolecules*, **30**, 526 (1997).
- [7] T. Inoue, D.S. Ryu, and K. Osaki, *Macromolecules*, **31**, 6977 (1998); M. Matsuyama, H. Watanabe, T. Inoue, and K. Osaki, *ibid.* **31**, 7973 (1998).
- [8] A. Kopf, B. Dünweg, and W. Paul, *J. Chem. Phys.*, **107** 6945 (1997).
- [9] K. Okun, M. Wolfhardt, J. Baschnagel, and K. Binder, *Macromolecules*, **30**, 3075 (1997).
- [10] C. Bennemann, J. Baschnagel, W. Paul, and K. Binder, *Comp. Theo. Poly. Sci.*, in print.
- [11] R. Yamamoto and A. Onuki, *Europhys. Lett.* **40**, 61 (1997); *Phys. Rev. E* **58**, 3515 (1998); A. Onuki and R. Yamamoto, *J. Non-Cryst. Solids*, **235** -**237**, 34 (1998).
- [12] R. Yamamoto and A. Onuki, *J. Phys. Soc. Jpn.*, **66** 2545 (1997); *Phys. Rev. Lett.* **81**, 4915 (1998).
- [13] M.P. Allen and D.J. Tildesley, *Computer Simulation of Liquids* (Clarendon, Oxford, 1987).
- [14] D.J. Evans and G.P. Morriss, *Statistical Mechanics of Nonequilibrium Liquids* (Academic, New York, 1990).
- [15] P.H. Verdier, *J. Chem. Phys.*, **45** 2118 (1966).
- [16] S. Chynoweth and Y. Michopoulos, *Molec. Phys.*, **81** 133 (1994).
- [17] R. Khare and J. de Pablo, *J. Chem. Phys.*, **107** 6956 (1997).
- [18] R. Muller, J.J. Pesce, and C. Picot, *Macromolecules*, **26**, 4356 (1993).